University of Baghdad
College of Engineering
JE
JOURNAL OF ENGINEERING

Journal of Engineering

journal homepage: www.jcoeng.edu.iq

Volume 32 Number 2 February 2026

Simulink Model for Monocrystalline Solar Panel Performance

Ahmed Hasan Dawood, Emad Talib Hashim*

Department of Energy Engineering, College of Engineering, University of Baghdad, Baghdad, Iraq

ABSTRACT

The present work evaluates the effects of different solar radiation values (350, 400, 650, 900, and 1000 W/m^2) and module temperature on the monocrystalline solar module output current, voltage, and power. A five-parameter model was chosen to design a simulation program to study and analyze the effects of irradiance and temperature on the output power of a solar module. Solar modules are defined by electrical factors like open circuit voltage, short circuit current, maximum power, maximum current, and maximum voltage, that not supplied by the manufacturer. The proposed work is suggested for the accurate determination model of a mono-crystalline solar module. Ideality factor calculation is by using the mathematical function, Lambert W function and series, and shunt resistances lead to extracting solar module parameters. The fitness of the five-factor formula is related to the lower RMSE average values. The average root mean square error of measured current-voltage values with the corresponding calculated values by the five-parameter model was calculated (0.0667). The lowest value of the root mean square errors of measured voltage-current characteristic values with the calculated ones is 0.022 at irradiance of 1000 W/m^2 and module operation temperature of 25 °C. Certainly will enhance the present work's fitness, represented by measured data or calculated model data with RMSE equal to 0.0667. It noted that the present work is so close to other important previous work, and that certainly enhances our work fitness (represented by measured data or calculated model data) with a 0.46 percentage of power drop per degree centigrade.

Keywords: Extracting, Lambert function, Power, Solar module temperature, Solar radiation

1. INTRODUCTION

Nowadays, electricity production is a critical problem all over the world because of population and industrial growth. Sustainable energy in its different forms is considered the main domain for electricity production **(Ma et al., 2014)**. Furthermore, photovoltaic solar energy is a significant trend in this field, clean and with no emissions to the environment **(Villalva et al., 2009)**. Today, more work has been done for different generation solar module systems **(Kosyachenko et al., 2014; Chatzisideris et al., 2016; Xu et al., 2017)**. Perovskite is the latest photovoltaic technology, due to its low price and high efficiency

*Corresponding author
Peer review under the responsibility of University of Baghdad.
https://doi.org/10.31026/j.eng.2026.02.03

Article received: 28/02/2025
Article revised: 10/11/2025
Article accepted: 26/11/2025
Article published: 01/02/2026

(Wang et al., 2015; Huang et al., 2015; Kung et al., 2015). Perovskite materials are key to achieving high solar module performance and activity, and numerous researchers strive to accomplish this **(Haider et al., 2020; Cui et al., 2014; Rahul et al., 2017)**. The first Pervoskite building was made by Tsutomu Miyasaka's Tokyo-based company with an efficiency of 2.2% in 2006 **(Kojima et al., 2006; Yusuf et al., 2024)**. Monomers of silicon crystalline are used in manufacturing solar crystalline modules. The purity of silicon gives these modules a uniform lock and recognizable shape **(Messenger and Abtahi, 2017)**. They manufactured a complete control system dependent on the Android control technique, and they also made a Simulink model using MATLAB functions. Many solar module parameter extraction methods are available in the literature. According to the intensive survey and especially for methods of extracting factors, one can classify these methods into analytic, iterative, and evolutionary computational methods **(Raseswari, 2013)**.

Huge work was done on extracting solar model parameters nonlinear fitting algorithm by **(Kim et al., 2010)**, approximate analytical methods by **(Das, 2012)**, and exact analytical methods by **(Bayhan et al., 2011)**, based on the Lambert W-function, which cannot be expressed in terms of basic functionalities. **(Ali et al., 2025a, b)** found the four-parameter model using different methods: slope method, and explicit simplified method. The accuracy of these methods, as it's compared with the measured data, is 5%, 7.9%, and 9.3%, respectively. **(Katia et al., 2021)** made experimental measurements for current, voltage, and power for two kinds of solar panels. These data were used to extract a four-parameter model using two different extraction methods. For monocrystalline solar panels, the percentage errors are 5% and 8% for the iterative method and simplified explicit, while for the corresponding copper indium gallium diselenide, they are 10% and 9%. More work concerned with modeling solar modules is available in these references **(Hussein and Hamzah, 2025; Cheng and Zhan, 2016)**.

The Lambert function is multivalued, namely the branches of the converse relation of the function $f(w) = we^w$, where w is any complex number and e^w is the exponential function. For each integer k, there is one branch, denoted by $W_k(z)$, which is a complex-valued function of one complex argument. W_0 is known as the principal branch **(Packel et al., 2004)**.

The scope of the work is to study the environmental conditions on solar panels, the variants of cell temperature, and their effectiveness on the I-V characteristic curve of PV solar modules. Also, to extract the five solar module parameters using the Lambert (w) function. To validate and check the simulation model outputs, the model results are compared with the corresponding measured data. The proposed work was done to obtain the best values for extracting the solar module parameters. According to the manufacturer's data sheet, photovoltaic properties, it is proven that it is necessary to calculate the five factors of the simulated electric circuit chosen for the solar module. The Lambert W function is used to estimate the solar panel's electric variables (I_{Ph}, I_o, R_S, R_{Sh},).

This method of parameter extraction uses simple parameter calculations in a simple method, and with very limited computation time. This simple procedure of calculation is reflected by a lower mean absolute error MAE, and the minimum of RMSE when compared to the other recent methods. It requires only the voltage and the current measured in the conditions of open circuit and short circuit, and the current and voltage of maximum power (MP).

The present proposed work is to calculate solar module electric variables based on the best and optimal estimation of the ideality factor value. Currently, the new and simple extraction methods are a challenge for researchers. A new approach is obtained to calculate mono-crystalline silicon cell five parameters. The present work aims to find the variables from the

ideality factor calculation using the Lambert function and the parasitic resistances curve (series and shunt). Absolute and relative errors are also calculated to show the proposed method over another method.

2. METHODOLOGY

A monocrystalline solar module is positioned just like in **Fig. 1**. The experimental work was conducted at the College of Engineering- Energy Department during a period of six months from January to June 2023. The experimental work was conducted under outdoor exposure in Baghdad- Al-Jaderia. The readings were taken within the time 9:00 AM-2:00 PM on selected days, where the atmospheric conditions of clear skies with no clouds, no dusty days, and no rain fell. To study the effect of temperature variations on solar performance, solar irradiance must be kept constant and vice versa. Therefore, to have the temperature range and for more accuracy, the measurements were done for the tested module with five solar radiation levels: 350, 400, 650, 900, and 1000 W/m^2.

The solar module analyzer (Prova 210) needs 10 seconds to make a scan with variable to supply the I-V and P-V characteristic curves, and this time at outdoor conditions is enough to have a constant solar radiation. The module is cleaned before the tests. The solar panel is fixed to the south direction with a tilted angle of 45 ^{o,} then record the temperature of the back side of the module (using a thermocouple) and start the IV scanning process, which is done by the Solar Module Analyzer, then save the data in a laptop. Solar panel and Prova 200 properties are available in **Tables 1 and 2,** respectively.

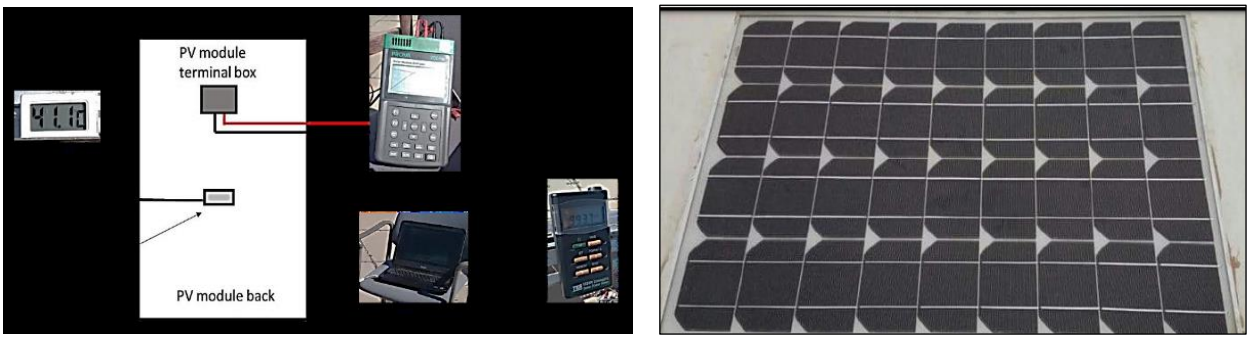

(a) (b)

Figure 1. Laboratory instruments: (a) system set up, (b) PV module.

Table 1. Monocrystalline silicon solar panel properties

Area, m^2	V_{oc}, V	I_{sc}, A	Peak power, W	Peak voltage, V	Peak current, A	No. of cells	Production data
0.46	21.6	3.24	50	17.44	2.88	36	2020

Table 2. Properties of solar panel analyzer (Prova 200)

Battery type	Rechargeable, 2500mAh (1.2V) x 8
AC adaptor	AC 110V or 220V input DC 12V / 1~3A output
Dimension	257(L) x 155(W) x 57(H) mm
Weight	1160g / 40.0oz (Batteries included)
Operation environment	0 °C ~ 50 °C , 85% RH
Temperature coefficient	0.1% of full scale / °C (＜18 °C or＞28 °C)

3. PHOTOVOLTAIC SYSTEM PARAMETERS EXTRACTION

The five-parameter model (**Van Dyk et al., 2004)** will be used at three operating conditions on the curve of I & V:

$$I = I_{pv} - I_0\left[exp\left(\frac{V+IR_s}{AV_T}\right) - 1\right] - \frac{V+IR_s}{R_p} \quad (1)$$

$Where \quad V_T = NkT/q$

The diode thermal voltage V_T, the Boltzmann constant K, the electron charge q, and solar cells connected in series N. The short-circuit operating point when V = 0

$$I_{sc} = I_{pv} - I_0\left[exp\left(\frac{I_{sc}R_s}{AV_T}\right) - 1\right] - \frac{I_{sc}R_s}{R_p} \quad (2)$$

The open–circuit operation point, V = V_{oc} and I = 0

$$0 = I_{pv} - I_0\left[exp\left(\frac{V_{oc}}{AV_T}\right) - 1\right] - \frac{V_{oc}}{R_p} \quad (3)$$

The open-circuit operating point, Vmp, and I = I_{mp}

$$I_{mp} = I_{pv} - I_0\left[exp\left(\frac{V_{mp}+I_{mp}R_s}{AV_T}\right) - 1\right] - \frac{V_{mp}+I_{mp}R_s}{R_p} \quad (4)$$

$$\frac{\partial I}{\partial V} = V\frac{\partial I}{\partial V} + I = 0 \quad (5)$$

Setting maximum power condition ($\frac{\partial p}{\partial V}$=0) to Eq. (5) will result in Eq. (6), which is obtained **(Sera et al., 2007)**

$$\frac{\partial I}{\partial V}|_{[I_{mp},V_{mp}]} = -\frac{I_{mp}}{V_{mp}} \quad (6)$$

$$\frac{dI}{dV} = -\frac{I_0}{AV_T}\left(1+\frac{dI}{dV}R_s\right)\left[exp\left(\frac{V+IR_s}{AV_T}\right)\right] - \frac{1}{R_p}\left(1+\frac{dI}{dV}R_S\right) \quad (7)$$

Neglecting the second term on the Eq. (1) in the right side **(Van Dyk et al., 2004)**:

$$I_{pv} = \frac{R_P+R_s}{R_P}I_{sc} \quad (8)$$

From Eqs. (2) and (7), the saturation current can be reduced **(Cubas et al., 2014)**

$$I_0 = \left(\left(R_p+R_s\right)I_{sc} - V_{oc}\right)/R_P\ exp\ exp\left(\frac{V_{oc}}{AV_T}\right) \quad (9)$$

Eq. (10) is attained from Eqs. (4), (8) and (9) **(Sera et al., 2007)**

$$I_{sc} - \left(I_{sc} - \frac{V_{oc}-R_sI_{SC}}{R_p}\right)\left[exp\left(\frac{V_{mp}+I_{mp}R_s-V_{oc}}{AV_T}\right)\right] - \frac{V_{mp}+I_{mp}-I_{sc}R_s}{R_p} = I_{mp} \quad (10)$$

From Eqs. (8) to (10) An implicit expression series resistance R_s is obtained **(Sera et al., 2007)**:

$$\frac{AV_T V_{mp}(2I_{mp}-I_{SC})}{\left(V_{mp}I_{sc}+V_{oc}(I_{mp}-I_{sc})\right)(V_{mp}-I_{mp}R_s)-AV_T(V_{mp}I_{sc}-V_{oc}I_{mp})} = exp\left(\frac{V_{mp}+I_{mp}R_s-V_{oc}}{AV_T}\right) \quad (11)$$

The R_p expression results from the combination of Eqs. (10) and (11) (**Sera et al., 2007)**:

$$R_P = \frac{\left(V_{mp}-I_{mp}R_s\right)\left(V_{mp}+R_s\left(I_{sc}-I_{mp}\right)\right)-AV_T}{\left(V_{mp}-I_{mp}R_s\right)\left(I_{sc}-I_{mp}\right)-aV_T I_{mp}} \quad (12)$$

Eq. (12) resolution and assisting of the Lambert (W) function **(Packel et al., 2004)** will have R_s series resistance

$$Z = W(z)e^{W(z)} \quad (13)$$

Where z is any complex number.
The Lambert w function has sub-function, the first $w_0(x)$ and the second $w_{-1}(x)$, **(Packel et al., 2004)**:

$$W(x) = \{W_o(x), \quad x \geq -1 \; W_{-1}(x), \quad x \leq -1 \quad (14)$$

$W(x) = \{Wo(x), x \geq -1 \; W-1(x), x \leq -1\}$

W domain:

- [-1/e, 0], the real variable x of of W(x) has a single image.
- X ≥ -1/e, the real variable x of w(x) has two images.

Lambert's W function in dealing with exponential formulas is to use the equivalence below **(Packel et al., 2004)**:

$$x = Ye^Y \leftrightarrow Y = W(x) \quad (15)$$

Eq. (11) can be written (**Sera et al., 2007)**

$$-\frac{V_{mp}\left(2I_{mp}-I_{sc}\right)}{\left(V_{mp}I_{sc}+V_{oc}\left(I_{mp}-I_{sc}\right)\right)} exp\left(-\frac{2V_{mp}-V_{oc}}{AV_T}+\frac{V_{mp}I_{sc}-V_{oc}I_{mp}}{V_{mp}I_{SC}+V_{oc}(I_{mp}-I_{sc}}\right)$$
$$= \left(\frac{I_{mp}R_s-V_{mp}}{AV_T}+\frac{V_{mp}I_{sc}-V_{oc}I_{mp}}{\left(V_{mp}I_{sc}+V_{oc}\left(I_{mp}-I_{sc}\right)\right)}\right) exp\left(\frac{I_{mp}R_s-V_{mp}}{mV_T}\right.$$
$$\left.+\frac{V_{mp}I_{SC}-V_{oc}I_{mp}}{\left(V_{mp}I_{sc}+V_{oc}\left(I_{mp}-I_{sc}\right)\right)}\right) \quad (16)$$

Using the Eqs. (15) and (16) becomes **(Sera et al., 2007):**

$$\frac{I_{mp}R_s - V_{mp}}{AV_T} + \frac{V_{mp}I_{sc} - V_{oc}I_{sc}}{V_{mp}I_{sc} + V_{oc}(I_{mp} - I_{sc})} = W_{-1}\left(-\frac{V_{mp}(2I_{mp} - I_{sc})}{(V_{mp}I_{sc} + V_{oc}(I_{mp} - I_{sc}))} exp\left(-\frac{2V_{mp} - V_{oc}}{AV_T} + \frac{V_{mp}I_{sc} - V_{oc}I_{mp}}{V_{mp}I_{SC} + V_{oc}(I_{mp} - I_{sc})}\right)\right) \quad (17)$$

From Eq. (17) we obtain R_s **(Sera et al., 2007)**:-

$$Rs = \frac{AV_T}{I_{mp}}\left(W_{-1}\left(-\frac{V_{mp}(2I_{mp}-I_{sc})}{(V_{mp}I_{sc}+V_{oc}(I_{mp}-I_{sc}))}\right) exp\left(-\frac{V_{mp}I_{sc}-V_{oc}I_{mp}}{V_{mp}I_{sc}+V_{oc}(I_{mp}-I_{sc})} - \frac{V_{mp}-V_{oc}}{AV_T} + \frac{V_{mp}I_{sc}-V_{oc}I_{mp}}{V_{mp}I_{sc}+V_{oc}(I_{mp}-I_{sc})}\right)\right) \quad (18)$$

4. MATLAB-SIMULINK MODEL OF PV SOLAR MODULE

Lambert W function **(Packel et al., 2004)** with the assistance of Matlab Simulink will be used to calculate the five factors of the PV panel at room temperature and pressure using a special program Matlab code that includes equations of each parameter and the data of the module at STC **(Hashim et al., 2018)**. A MATLAB-SIMULINK model of a PV solar module will study the influence of different values of solar radiation on the corresponding solar module operation temperature, and also study the effect of wind velocity on the temperature of the PV solar module by using a Simulink block diagram. The basis for a Simulink model is the mathematical equations representing a given system **(Hashim et al., 2018)**. This final Simulink illustrates measured (I_{PV},V_{PV}, P_{PV}) in this model and the scope model used to plot the graph. The simulation modelling of the solar module measured the value of five parameters ($I_{Ph}, I_o, R_S, R_{Sh}, A$) and operating temperature when inputting the value of (radiation, ambient temperature, wind speed) that was measured in experimental work is shown in **Fig. 2 a and b** (our present modelled Simulink).

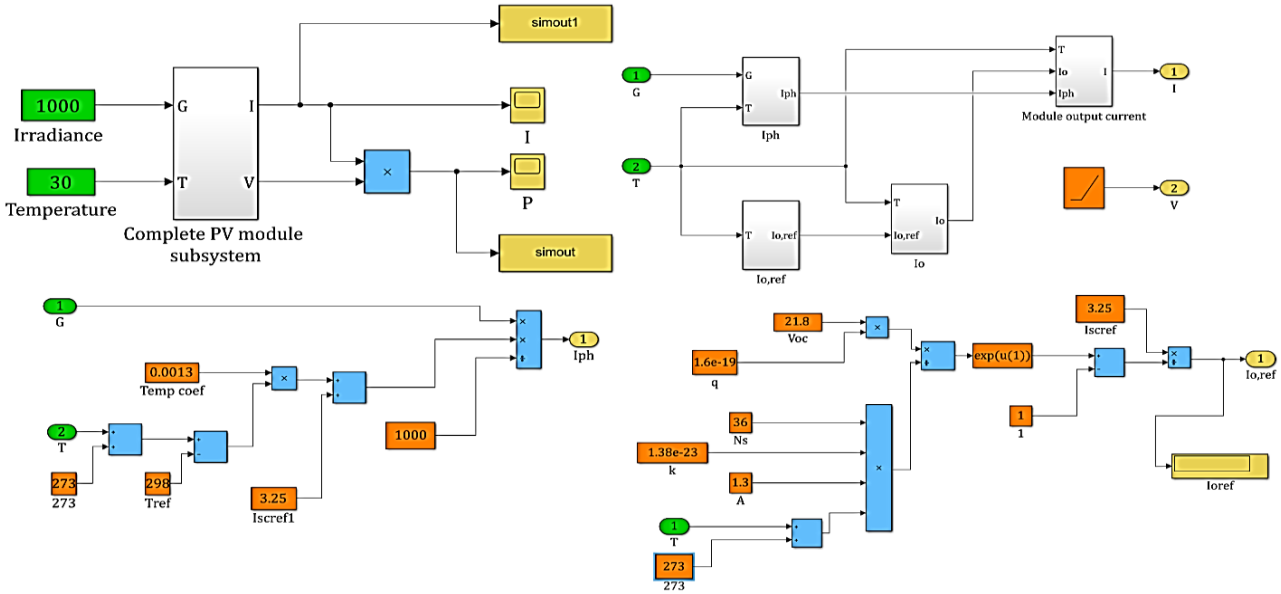

(a)

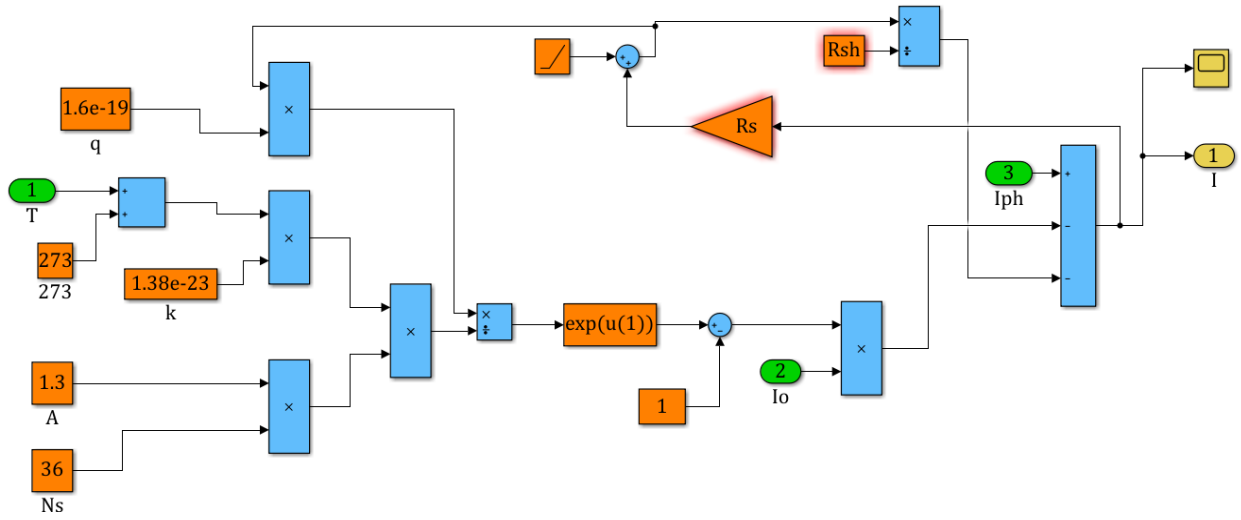

(b)

Figure 2. Simulink model for panel modeling: a. factor model b. Simulink model using a five-factor model.

5. CASE STUDY

A monocrystalline panel is chosen to examine the present work since its I-V data were measured at standard testing conditions (STC) (solar radiation of 1000 W/m^2 and room temperature of 25°C) and other testing conditions. These other testing conditions are the solar radiations: 350, 400, 650, 900, 1000, and 1000 W/m^2 with corresponding solar module operating temperatures: 23, 42, 32, 45, 38, 52 ^{o}C, respectively. The solar panel has 36 series solar cells. The range of calculated values of the ideality factor is 1.25-1.4, see **Table 3**. Worth noting that the value of the ideality factor for a semiconductor varies from 1 to 2.
In the present work, it is suggested to work within a closed ideality factor of 1.25-1.4, which is more suitable for mono-crystalline silicon semiconductor.

Table 3. The variable calculated for the ideality factor

	Reference	Test 1	Test 2	Test 3	Test 4	Test 5	Test 6
Radiation, W/ m^2	1000	1000	1000	350	400	650	900
Temperature, ^{o}C	25	52	38	23	42	32	45
I_{ph}, A	3.240	3.240	3.240	1.135	1.296	2.100	2.920
I_o, A*10^7	0.515	2.2	1.15	4.56	1.35	7.7	1.59
A	1.4	1.36	1.4	1.25	1.27	1.29	1.37
R_s, Ω	0.270	0.387	0.357	0.924	0.883	0.525	0.410
R_{sh}, Ω	103.3	110.7	105.8	286.0	256.1	158.3	118.7

6. ACCURACY OF FIVE-PARAMETER MODEL

An Excel sheet has the measured and calculated data at five radiation levels over six months, and aims to find out the fitness between the measured data and the corresponding extracted ones. Eq. (19) gives the percentage of error between the measured values and calculated values (Matlab Simulink) **(Hashim et al., 2018)**:

$$\frac{Matlab\ Simulink - Laboratory\ measurments}{Laboratory\ measurments} \times 100\% \quad (19)$$

Table 4 contains the measured operating solar module temperatures and solar module efficiencies at the five tested solar irradiance levels: 350, 400, 650, 900, and 1000 Wm^{-2}. This table shows that the lowest solar efficiency is 9.7% and the highest is 11.8%. The maximum power is attained at the highest solar radiation, 1000 $Wm^{-2,}$ and the corresponding solar module temperature is 25 °C at fixed solar irradiance. Decreasing solar module temperature will lead to an increase in efficiency and power output. That is due to a decrease in reverse saturation current.

Table 4. Comparisons between measured data and the five-parameter model result at the five tested irradiance levels: 350, 400, 650, 900, 1000 Wm^{-2}.

Solar radiation, Wm^{-2}	**350**	**400**	**650**	**900**
$T_{C,\,exp.}, {}^{o}C$	17	25	33	45
$\eta_{exp\,l.}, W$	11.8	10.8	10.0	9.7
$P_{m,exp.}, W$	16.93	17.02	32.94	39.53
$P_{m,cal}, W$	14.52	15.21	29.16	36.60
Error, %	-14.2	-10.6	-11.5	-7.4
$I_{m,exp.}, W$	1.042	1.146	1.986	2.606
$I_{m,cal.}, W$	0.968	1.056	1.798	2.440
Error, %	-7.1	7.8	9.4	-6.4
$V_{m,exp.}, W$	16.249	14.85	16.59	15.17
$V_{m,cal}, W$	15.00	14.40	16.30	15.00
Error, %	-7.7	-4.5	-2.9	-1.1
Solar radiation, Wm^{-2}	**1000**	**1000**	**1000**	
$T_{C,\,exp.}, {}^{o}C$	25	38	52	
$\eta_{exp\,l.}, W$	9.9	10.1	9.8	
$P_{m,exp.}, W$	50.15	45.55	43.38	
$P_{m,cal}, W$	50.75	47.32	43.38	
Error, %	-1.2	-3.9	0.0	
$I_{m,exp.}, W$	2.705	2.872	2.698	
$I_{m,cal}, W$	2.769	2.915	2.698	
Error, %	-0.2	1.5	0.0	
$V_{m,exp.}, W$	18.327	15.86	16.08	
$V_{m,cal}, W$	17.95	16.234	16.08	
Error, %	-3.5	2.3	0.0	

7. RESULTS AND DISCUSSION

Figs. 3 to **9** give the I-V characterization curves given by the Simulink calculation, with the corresponding measured ones. This model summarizes to good results but reflects poor output results at low solar irradiance.

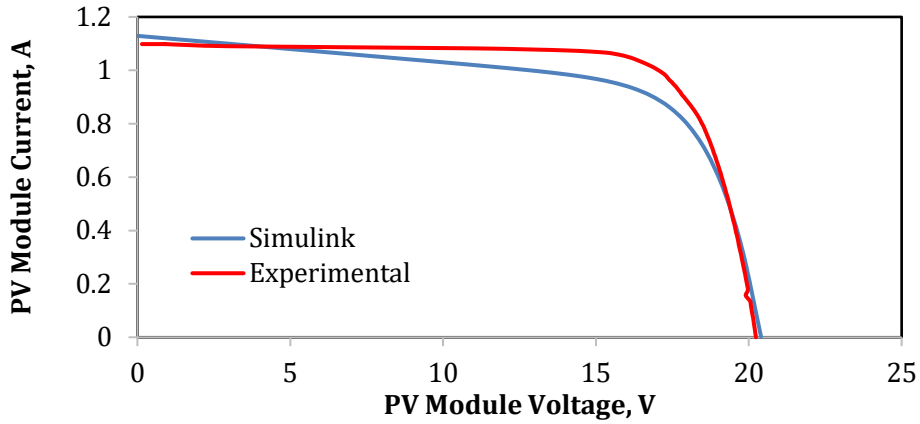

Figure. 3 Measured and calculated I-V characteristic curve of monocrystalline solar panel at irradiance 350 W m^{-2} and temperature 23 °C

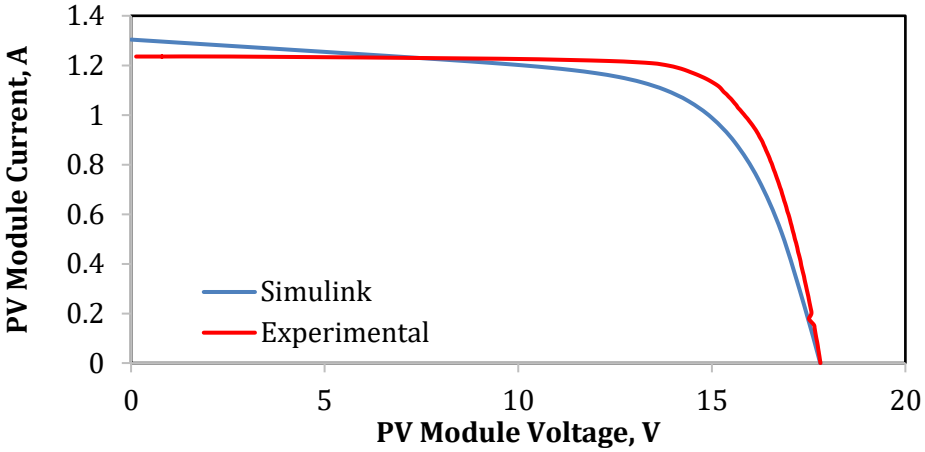

Figure 4. Measured and calculated I-V characteristic curve of monocrystalline solar panel at irradiance 400 W m^{-2} and temperature 42 °C

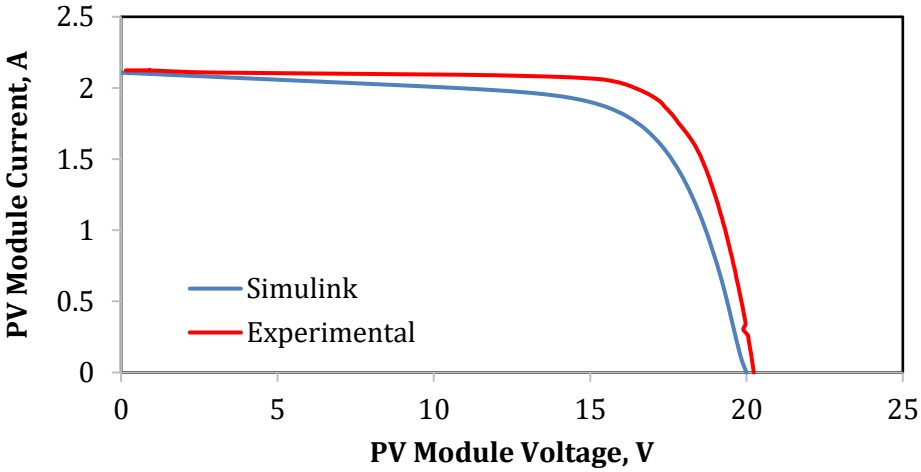

Figure 5. Measured and calculated I-V characteristic curve of a monocrystalline solar panel at irradiance 650 W m^{-2} and temperature 32 °C

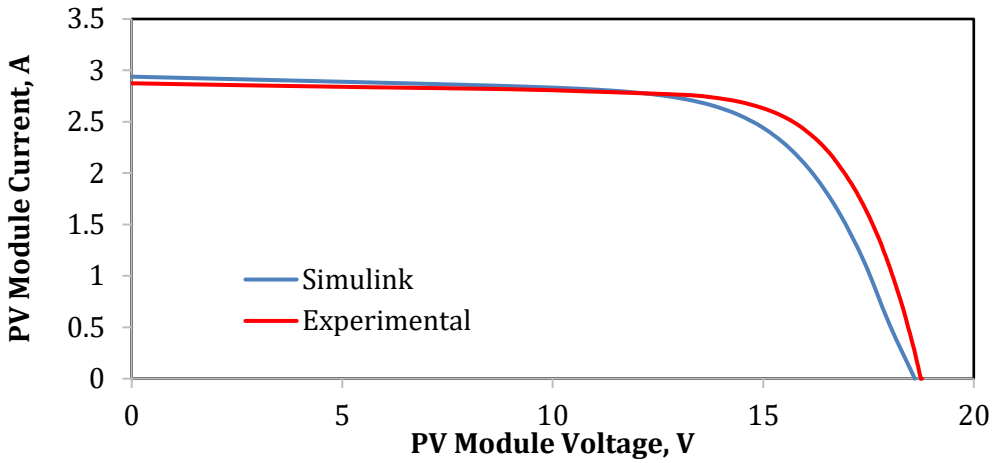

Figure 6. Measured and calculated I-V characteristic curve of a monocrystalline solar panel at irradiance 900 W m^{-2} and temperature 45 °C

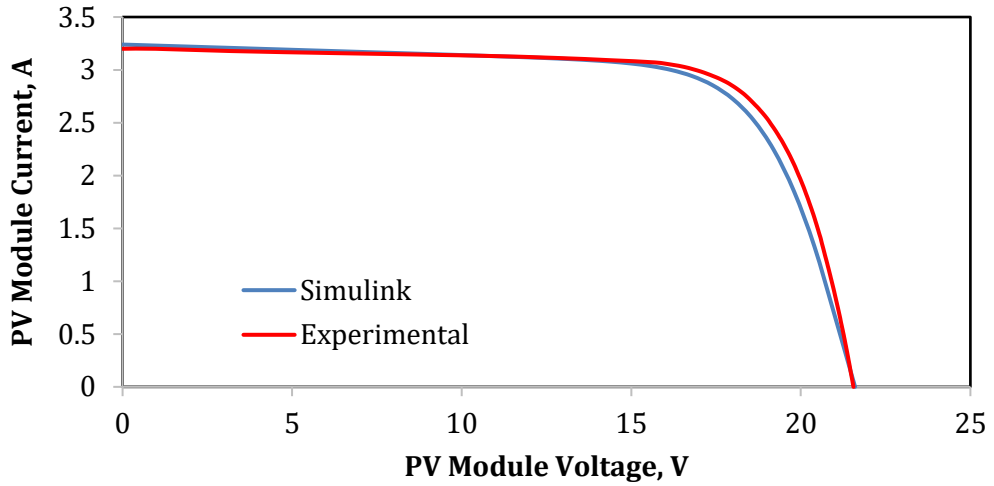

Figure. 7 Measured and calculated I-V characteristic curve of monocrystalline solar panel at irradiance 1000 W m^{-2} and temperature 25 °C

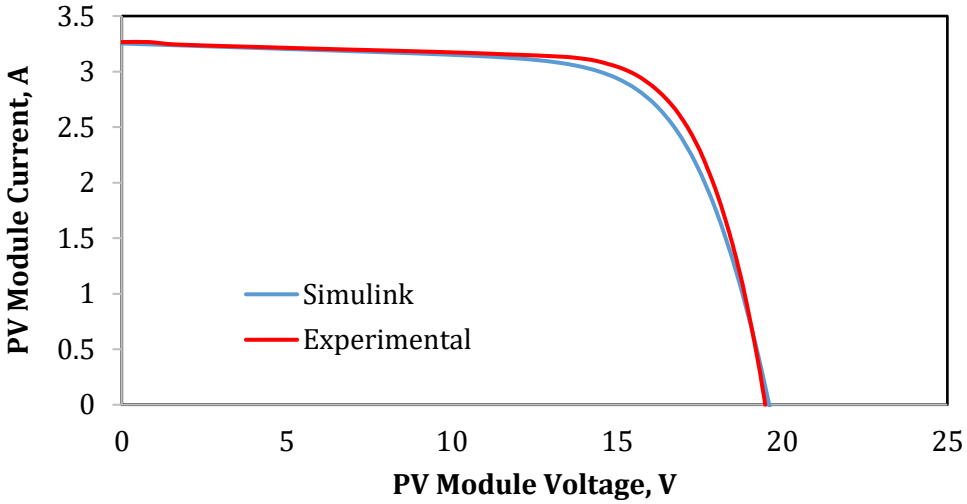

Figure 8. Measured and calculated I-V characteristic curve of monocrystalline solar panel at irradiance 1000 W m^{-2} and temperature 38 °C

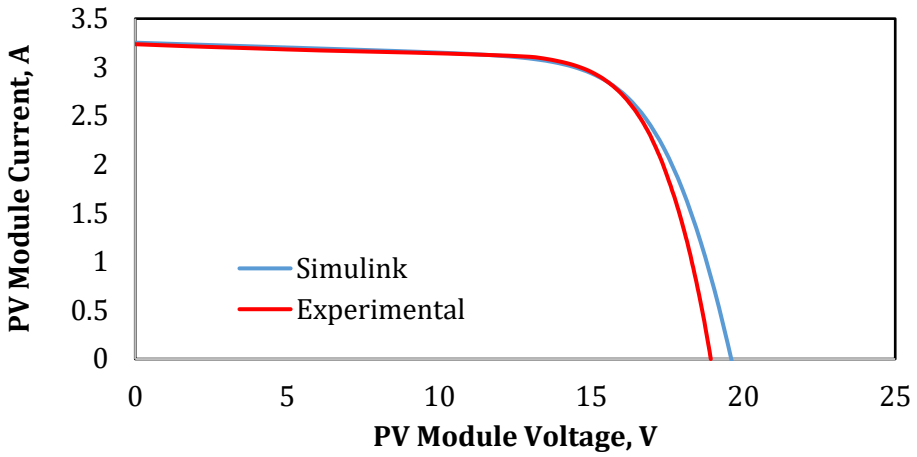

Figure 9. Measured and calculated I-V characteristic curve of monocrystalline solar panel at irradiance 1000 W m^{-2} and temperature 52 °C

Statistical work was done to calculate root mean square error (RMSE) (**Ma and Iqbal, 1984)**:

$$RMSE = (\frac{1}{n}\sum_{j=1}^{n}(I_{si} - I_{mi})^2)^{\frac{1}{2}} \quad (20)$$

Where n is the number of data, I_{si} is the i_{th} simulated current, and I_{mi} is the i_{th} measured current. The RMSE satisfies and evaluates the accuracy of the simulated model. The more accurate the formula (model) corresponds to low values of RMSE. **Fig. 3** shows the experimental current value and the Simulink current calculated value against the corresponding voltage values at solar radiation 350 W/m^2 and module operating temperature 23 °C. It is noted that close-fitting values at the terminals between the measured and calculated (Simulink) ones, while more deviation is observed in other curve zones. This behavior approximately continued in **Fig. 4,** like **Fig. 3,** with solar radiation of 400 W/m^2 and module operating temperature of 42 °C. **Fig. 5** summarized the measured and calculated I-V characteristic curve of the solar panel at irradiance 650 W m^{-2} and temperature 32 °C. **Fig. 5** shows that all the calculated current values are lower than the measured one, which explain that the Simulink model has a negative prediction of measured current values. **Fig. 6** shows the measured and calculated I-V characteristic curve of a monocrystalline solar panel at irradiance 900 W m^{-2} and temperature 45 °C. **Fig. 7:** the measured and calculated I-V characteristic curve of the module at irradiance 1000 W m^{-2} and temperature 25 °C. For these two figures (**Figs. 6 and 7**), the obtained results (calculated and measured ones) are so close to each other. It can be concluded that the model gives closer results in higher solar radiation,900 and 1000 W m^{-2}. **Table 5** gives the estimated values of RMSE from the model. The fitness of the five-factor model is related to the lower RMSE average values. At solar radiation 1000 W/m^2 (Test 5), the RMSE value is 0.022. That means the closed I-V measured and the I-V simulated are compared to each other.

Table 5. RMSE for the seven tested cases

	Test 1	**Test 2**	**Test 3**	**Test 4**	**Test 5**	**Test 6**	**Test 7**
G, Wm^{-2}	350	400	650	900	1000	1000	1000
Tc, ^{o}C	23	42	23	45	25	38	52
RMSE	0.109	0.116	0.103	0.069	0.022	0.023	0.026

A linear relationship exists between solar radiation and solar panel output power. Also, there is linear proportionality between solar radiation and PV module short circuit current (I_{sc}) (see **Table 6,** tests 1, 3, 4, and 5 for measured I_{sc}). An exponential proportionality between solar radiation and open circuit voltage (V_{oc}), and its values change slightly with the intensity of solar irradiance values (See **Table 6** tests 5, 6, and 7 for the measured V_{oc}).
Atmospheric temperature has a direct effect on the solar panel's operating temperature. Solar module temperature increases lead to a very small increase in short-circuit current. However, open circuit voltage is extremely affected by increasing solar panel temperature to more than 25 °C. In other words, the increasing current is proportionally lower than the decreasing voltage. So, it is clear that low solar module performance and power occur with increasing operating solar module temperature (See **Table 6** tests 5, 6, and 7 for the measured power values). **Table 7** summarizes comparisons with some previous works available in the literature for the maximum power drop. It is noted that the present work is so close to other important previous work, and that certainly enhances our work's fitness (represented by measured data or calculated model data)

Table 6. Measured and calculated V_{oc} and I_{sc} for the seven tested cases

Test No.	G, Wm^{-2}	T_c, °C	V_{oc}, V			I_{sc}, A		
			measured	calculated	error, %	measured	calculated	error, %
1	350	23	20.234	20.400	0.8	1.097	1.129	2.9
2	400	42	17.806	17.800	0.0	1.236	1.304	5.5
3	650	32	20.234	20.000	-1.1	2.112	2.107	-0.5
4	900	45	18.772	18.617	-0.8	2.874	2.939	2.3
5	1000	25	21.552	21.606	0.3	3.199	3.239	1.2
6	1000	38	19.484	19.804	1.6	3.256	3.253	0.0
7	1000	52	18.933	19.778	-4.4	3.237	3.253	1.6

Table 7. Maximum power drop comparisons with some previous work.

Study case	**Present study**	**(Hashim et al., 2016)**	**(Radziemska, 2002)**	**(Buday, 2011)**
%/ºC	0.46	0.45	0.65	0.5
Study case	**(El-Shaer et al., 2014)**	**(Spataru et al., 2014)**	**(Dash and Gupta, 2015)**	
%/°C	0.25	0.4546	0.446	

8. CONCLUSIONS

The present work was done to find the best values for extracting the solar panel parameters. According to the manufacturer's data sheet, photovoltaic properties, it is proven is necessary to calculate the five factors of the equivalent circuit model chosen for the solar module. The Lambert W function allowed us to have access to solar module parameter extraction ($I_{Ph}, I_o, R_S, R_{Sh}, A$). The Lambert-W function helped us to develop explicit functions for parameter calculations. The fitness of the five-parameter model is related to the lower RMSE average values. The average root mean square error of measured current-voltage values with the corresponding calculated values by the parameter model was calculated (0.0667). It is noted that the present work is so close to other important previous work, and that certainly enhances our work's fitness (represented by measured data or calculated model data). It is

recommended to study the modeling in different models, such as two-diode or three-diode models, and make a comparison between them.

NOMENCLATURE

Symbol	Description	Symbol	Description
A	diode ideality factor, dimensionless.	q	electron charge, 1.6×10^{-19} coulombs
I	output current of the solar module, A.	T	temperature, ^{o}C
I_m	current at maximum power point, A.	V	output voltage of the solar module, V
I_o	diode current, A	V_m	voltage at maximum power point, V
I_{ph}	solar-generated current, A	V_{oc}	open circuit voltage, V
I_{pv}	output current, A	V_T	diode thermal voltage, V
I_s	diode current saturated, A	R_p	parallel resistance, Ω
I_{sc}	short circuit current, A	R_s	series resistance, Ω
K	Boltzmann constant $1.3805*10^{-23}$ (Joule/k)	R_{sh}	shunt resistance, Ω
N	No. of solar cell connected in series	η	solar cell efficiency, %

Credit Authorship Contribution Statement

Ahmed Hasan Dawood: Experimental work, Writing, Validation, Methodology. Emad Talib Hashim: Review and editing, Validation, Proofreading.

Declaration of Competing Interest

The authors declared that they have no known competing financial interests or personal relationships that would have appeared to influence the work reported in this article.

REFERENCES

Ali M. Rasham and Mohammed A. Nima, 2025a. Performance improvement of air-based photovoltaic thermal solar systems through innovative metallic foam configurations within converging ducts. *Results in Engineering* 28, P. 107232. https://doi.org/10.1016/j.rineng.2025.107232

Ali M. Rasham and Mohammed A. Nima, 2025b. Comprehensive analysis of the thermoelectrical performance of an air-based photovoltaic thermal solar collector integrated with innovative gridded metal foams. Results in Engineering 27, P. 105826. https://doi.org/10.1016/j.rineng.2025.105826

Ahmed, M. A., and Mohamed, H., 2020. Exploring the potential of solar, tidal, and wind energy resources in Oman using an integrated climatic-socioeconomic approach. *Renewable energy*, 161, pp. 662-675. https://doi.org/10.1016/j.renene.2020.07.144

Bayhan, H., and Bayhan, M., 2011. A simple approach to determine the solar cell diode ideality factor under illumination. *Solar Energy*, 85(5), pp. 769–775. https://doi.org/10.1016/J.SOLENER.2011.01.009.

Buday, M. S., 2011. Measuring irradiance, temperature, and angle of incidence effects on photovoltaic modules in Auburn Hills, *Michigan*. Thesis for Master of Science/Sustainable Systems (Natural Resources and Environment) at the University of Michigan.

Chatzisideris, M. D., Espinosa, N., Laurent, A., and Krebs, F. C., 2016. Ecodesign perspectives of thin-film photovoltaic technologies: A review of life cycle assessment studies. *Solar Energy Materials and Solar Cells*, 156, pp. 2-10. https://doi.org/10.1016/j.solmat.2016.05.048

Cheng, P., and Zhan, X., 2016. Stability of organic solar cells: Challenges and strategies. Chemical Society Reviews, 45(9), pp. 2544-2582. https://doi.org/10.1039/C5CS00593K

Cui, J., Meng, F., Zhang, H., Cao, K., Yuan, H., Cheng, Y., Huang, F., and Wang, M., 2014. $CH_3NH_3PbI_3$-based planar solar cells with magnetron-sputtered nickel oxide. *ACS applied materials & interfaces*, 6(24), pp. 22862-22870. https://doi.org/10.1021/am507108u

Javer, C., Santiago, P., and Carlos, M., 2014. Explicit Expressions for Solar Panel Equivalent Circuit Parameters Based on Analytical Formulation and the Lambert W-Function. *Energies*, pp. 4098-4115. https://doi.org/10.3390/en7074098.

El-Shaer, A., Tadros, M. T. Y., and Mohamed, A. K., 2014. Effect of Light Intensity and Temperature on Crystalline Silicon Solar Modules Parameters. *International Journal of Emerging Technology and Advanced Engineering,* 4(8), pp. 311.http://doi.org/ 16557433/2014

Haider, M., Yang, JL 2020. Efficient and stable perovskite–silicon two-terminal tandem solar cells. *Rare Met.* 39, pp. 745–747. https://doi.org/10.1007/s12598-020-01430-4

Hahsim, E.T., 2016. Determination of Mono-crystalline Silicon Photovoltaic Module Parameters Using Three Different Methods. *Journal of Engineering*, 22(7), pp. 92-107.https://doi.org/10.31026/j.eng.2016.07.06

Hashim, E. T., and Talib, Z. R., 2018. Study of the performance of the five-parameter model for a monocrystalline silicon photovoltaic module using reference data .*FME Transactions*, 46, pp. 585-594. https://doi.org/10.5937/fmet1804585T

Hussein, H. S., and Hamzah A. A., 2025. Study of heat generation and power losses in MultiCrystalline Silicon photovoltaic solar module. *Journal of Engineering*, 31(10), pp. 65–85. https://doi.org/10.31026/j.eng.2025.10.04.

Huang, Z., Xu, W., and Yu, K. 2015. Bidirectional LSTM-CRF models for sequence tagging. *arXiv preprint arXiv:1508.01991*. https://doi.org/10.48550/arXiv.1508.01991

Katee, N. S., Abdullah, O. I., and Hashim, E. T. 2021. Extracting four solar model electrical parameters of mono-crystalline silicon (mc-Si) and thin film (CIGS) solar modules using different methods. *Journal of Engineering*, 27(4), pp. 16-32. https://doi.org/10.31026/j.eng.2021.04.02

Kim, W., and Choi, W., 2010. A novel parameter extraction method for the one-diode solar cell model. *Solar Energy*, 84(6), pp. 1008–1019. https://doi.org/10.1016/j.solener.2010.03.012.

Kosyachenko, L. A., Mathew, X., Paulson, P. D., Lytvynenko, V. Y., and Maslyanchuk, O. L. 2014. Optical and recombination losses in thin-film Cu (In, Ga) Se2 solar cells. *Solar energy materials and solar cells*, *130*, pp. 291-302. https://doi.org/10.1016/j.solmat.2014.07.019

Kojima, A., Teshima, K., Shirai, Y., and Miyasaka, T. 2009. Organometal halide perovskites as visible-light sensitizers for photovoltaic cells. *Journal of the American Chemical Society*, *131*(17), pp. 6050-6051. https://doi.org/10.1021/ja809598r

Kung, J. T., Kesner, B., An, J. Y., Ahn, J. Y., Cifuentes-Rojas, C., Colognori, D., Jeon, Y., Szanto, A., del Rosario, B. C., Pinter, S. F., Erwin, J. A., and Lee, J. T. 2015. Locus-specific targeting to the X chromosome revealed by the RNA interactome of CTCF. *Molecular Cell*, *57*(2), pp. 361-375. https://doi.org/10.1016/j.molcel.2014.12.006

Ma, C.C.Y., and Iqbal, M., 1984. Statistical comparison of solar radiation correlations, monthly average global and diffuse radiation on horizontal surfaces. *Solar Energy*, pp. 143-148. https://doi.org/10.1016/0038-092X(84)90231-7.

Ma, T, Yang, H. and Lu, L., 2014. Solar photovoltaic system modeling and performance prediction. Renew Sustain *Energy Rev, 36*, pp. 4–15. https://doi: 10.1016/j.rser.2014.04.057.

Messenger, R. A., and Abtahi, H. A., 2017. Photovoltaic Systems Engineering, Third edition, CRC Press, Boca Raton, Florida, pp.21-30.

Packel, E. and Yuen, D., 2004. Projectile Motion with Resistance and the Lambert Function. *College Math. J.,* 35, pp. 337-350. https://doi.org/10.1007/s10910-018-0985-3

Parbar K. D., and Gupta, N. C., 2015. *Effect of Temperature on Power Output from Different Commercially Available Photovoltaic Modules*. Journal of Engineering Research and Applications, 5(1) (Part 1), pp. 148-151.

Radziemska, E., and Klugmann, E., 2002. Thermally affected parameters of the current–voltage characteristics of the silicon photocell. *Energy Conversion and Management*. 43(14), pp. 1889-1900. https://doi.org/10.1016/S0196-8904(01)00132-7.

Rahul, Abhishek, K., Datta, S., Biswal, B. B., and Mahapatra, S. S., 2017. Machining performance optimization for electro-discharge machining of Inconel 601, 625, 718, and 825: An integrated optimization route combining satisfaction function, fuzzy inference system, and Taguchi approach. *Journal of the Brazilian Society of Mechanical Sciences and Engineering*, *39*, pp. 3499-3527. https://doi.org/10.1007/s40430-016-0659-7

Raseswari, P., 2013. Development of New Parameter Extraction Schemes and Maximum Power Point Controllers for Photovoltaic Power Systems. PhD thesis, National Institute of Technology Rourkela.

Sera, D., Teodorescu, R, and Rodriguez, P., 2007. PV panel model based on datasheet values. *IEEE International Symposium on Industrial Electronics*, Vigo (Spain), pp. 2392-2396. https://doi.org/10.1109/ISIE.2007.4374981.

Shao, Y., Zheng, D., Liu, L., Liu, J., Du, M., Peng, L., and Liu, S. 2024. Innovations in interconnecting layers for perovskite-based tandem solar cells. ACS Energy Letters, 9(10), pp. 4892-4921. https://doi.org/10.7498/aps.73.20241187

Spataru, S., Sera, D., Kerekes, T., Teodorescu, R., Cotfas, P. A., and Cotfas, D. T., 2014. Experiment based teaching of solar cell operation and characterization using the SolarLab platform. In *Proceedings of the 7th International Workshop on Teaching in Photovoltaics* (Vol. 7). Czech Technical University in Prague, Faculty of Electrical Engineering.

Van Dyk, E. E., and Meyer, E. L., 2004. Analysis of the effect of parasitic resistances on the performance of photovoltaic modules. *Renewable Energy*, 29, pp. 333-334. https://doi.org/10.1016/S0960-1481(03)00250-7.

Villalva, M. G., Gazoli, J. R., and Filho, E. R., 2009. Comprehensive Approach to Modeling and Simulation of Photovoltaic Arrays. *IEEE Trans. Power Electron.*, 24(5), pp. 1198–1208. https://doi.org/10.1109/TPEL.2009.2013862.

Wang, W., Arora, R., Livescu, K., and Bilmes, J., 2015. On deep multi-view representation learning. In *International Conference on machine learning*, pp. 1083-1092. PMLR. https://dl.acm.org/doi/10.5555/3045118.3045234

Xu, X., Zhao, Y., Sima, J., Zhao, L., Mašek, O., and Cao, X., 2017. Indispensable role of biochar-inherent mineral constituents in its environmental applications: A review. *Bioresource Technology*, *241*, pp. 887-899. https://doi.org/10.1016/j.biortech.2017.06.023

Yusuf, A. S., Ramalan, A. M., Abubakar, A. A., and Mohammed, I. K. 2024. Effect of Electron Transport Layers, Interface Defect Density, and Working Temperature on Perovskite Solar Cells Using SCAPS 1-D Software. *East European Journal of Physics*, (1), pp. 332-341. https://doi.org/10.26565/2312-4334-2024-1-31

تحديد معاملات الوحدة الكهروضوئية المصنوعة من السيليكون أحادي البلورة باستخدام طريقة لامبرت

احمد حسن داوود ، عماد طالب هاشم*

قسم هندسة الطاقة، كلية الهندسة، جامعة بغداد، بغداد، العراق

الخلاصة

يقيم العمل الحالي تأثير قيم الإشعاع الشمسي المختلفة 350 و 400 و 650 و 900 و 1000 واط / متر مربع ودرجة حرارة الوحدة على تيار خرج الوحدة الشمسية أحادية البلورة والجهد وأداء الطاقة. تم اختيار نموذج بخمسة معاملات لتصميم برنامج محاكاة لدراسة وتحليل تأثير الإشعاع ودرجة الحرارة على طاقة خرج الوحدة الشمسية. يتم تعريف الوحدات الشمسية من خلال العوامل الكهربائية مثل جهد الدائرة المفتوحة وتيار الدائرة القصيرة والقدرة القصوى والتيار الأقصى والجهد الأقصى، والتي لا يوفرها المصنع. تم اقتراح العمل المقترح لنموذج التحديد الدقيق للوحدة الشمسية أحادية البلورة. يتم حساب عامل المثالية باستخدام الدالة الرياضية ودالة لامبرت W والسلسلة ومقاومات التحويلة تؤدي إلى استخراج معلمات الوحدة الشمسية. ترتبط ملاءمة صيغة العوامل الخمسة بقيم متوسط RMSE المنخفضة. تم حساب متوسط خطأ الجذر التربيعي المتوسط لقيم التيار والجهد المقاسة مع القيم المحسوبة المقابلة بواسطة نموذج الخمسة معلمات (0.0667). أقل قيمة لجذر متوسط مربعات الأخطاء لقيم خصائص الجهد–التيار المقاسة مع القيم المحسوبة هي 0.022 عند إشعاع 1000 واط/م² ودرجة حرارة تشغيل الوحدة 25 درجة مئوية. سيعزز هذا بالتأكيد ملاءمة العمل الحالي، ممثلةً بالبيانات المقاسة أو بيانات النموذج المحسوبة، مع معامل تربيع متوسط يساوي 0.0667. وقد لوحظ أن هذا العمل قريب جدًا من أعمال سابقة مهمة أخرى، وهذا بالتأكيد يعزز ملاءمة عملنا (ممثلةً بالبيانات المقاسة أو بيانات النموذج المحسوبة) بنسبة 0.46% من انخفاض القدرة لكل درجة مئوية.

الكلمات المفتاحية: استحصال، داله لامبرت، قدرة، درجة حرارة اللوح الشمسي، الاشعاع الشمسي